Review Article

Separation anxiety: Stress, tension and cytokinesis

Krithika Mohan[a], Pablo A. Iglesias[a,*], Douglas N. Robinson[b,**]

[a]Department of Electrical & Computer Engineering, The Johns Hopkins University, 3400 N. Charles Street, Baltimore, MD 21218, USA
[b]Department of Cell Biology, Johns Hopkins University School of Medicine, 725 N. Wolfe Street, Baltimore, MD 21205, USA

ARTICLE INFORMATION

ABSTRACT

Cytokinesis, the physical separation of a mother cell into two daughter cells, progresses through a series of well-defined changes in morphology. These changes involve distinct biochemical and mechanical processes. Here, we review the mechanical features of cells during cytokinesis, discussing both the material properties as well as sources of stresses, both active and passive, which lead to the observed changes in morphology. We also describe a mechanosensory feedback control system that regulates protein localization and shape progression during cytokinesis.

© 2012 Elsevier Inc. All rights reserved.

Contents

 * Corresponding author. Fax: +1 410 516 5566.
 ** Corresponding author. Fax: +1 410 955 4129.
    E-mail addresses: pi@jhu.edu (P.A. Iglesias), dnr@jhmi.edu (D.N. Robinson).

Introduction

Cell shape changes form a fundamental step in many developmental processes, including tissue morphogenesis and organogenesis. Deformation and reformation of cell morphology require physical forces acting on the cell's physical material, all under the regulation of biochemical signaling pathways. Identifying the mechanical properties of cells and unveiling the molecular mechanisms driving shape changes are a great challenge in the field of cell and tissue morphogenesis. A first step is to understand the mechanics behind one of the simplest cell shape change processes, cytokinesis. Cytokinesis is a dynamic morphogenetic process that is carefully regulated so as to occur only after the chromosomes have separated through processes discussed in detail in other articles in this Special Issue on Chromosome Biology. During cytokinesis, the mother cell's cytoskeletal network is remodeled as the nuclear and cytoplasmic contents are (typically) evenly distributed into two hemispheres from which the daughter cells emerge. Understanding the mechanisms of this simple but yet dramatic shape change calls for the integration of principles from cell biology, mathematics, physics and engineering.

Cell rounding before cleavage furrow formation

Sometime between entry into mitosis and anaphase, the cell typically rounds up in preparation for cleavage furrow formation and contraction (Fig. 1A). In some systems, this morphological change is accompanied by a reduction in mechanical deformability, owing to an increase in cortical tension and/or rigidity [1–6]. The molecular basis for these morphological and mechanical changes is suggested from studies in multiple systems. In *Dictyostelium*, the rounding process occurs coordinately with the redistribution of several proteins. The actin binding proteins dynacortin and coronin as well as PH-Crac (which serves as a reporter of PI(3,4,5)P$_3$) move off of the cortex and membrane, whereas myosin II and PTEN phosphatase coordinately move onto the cortex and membrane [7,8]. Consistently, in mammalian cells, RhoA activity rises during this mitotic rounding phase and is needed to increase the apparent rigidity of the mitotic cells [9]. These changes in protein distributions correlate with changes in hydrostatic pressure, which are also thought to help drive the rounding event [10]. Furthermore, in echinoderm eggs, an increase in myosin II-contractility regulated by a global increase in myosin II light chain kinase activity has been observed [6].

The three phases of cleavage furrow ingression

Once the cells have rounded, they then pass through a series of highly stereotypical shape changes. In *Dictyostelium*, this shape evolution can be separated into three distinct phases (Fig. 1A) [11,12]. The first phase involves the movement of the cell away from equilibrium as the round mother cell (mitotic *Dictyostelium* cells have a ~5-μm radius) elongates into a prolate ellipsoid (with a ~8 μm diameter and ~12 μm length). During this phase, myosin II begins to accumulate along the central 25% of the cell. As the furrow ingresses, myosin II progressively concentrates, reaching a furrow-to-pole ratio of ~2–2.5. Yet, the peak total myosin amount

corresponds to the point at which the furrow just begins to ingress further than the daughter cell cortex [13,14]. This point when the total myosin II peaks marks the transition between Phases 1 and 2. During Phase 2, another transition occurs in which the furrow reaches the point where its length and diameter are equivalent; this point is referred to as the cross-over point (D_x). For wild type adherent *Dictyostelium* cells, the transition through the cross-over is smooth without a dramatic change in the furrow ingression dynamics. Thereafter, the trajectory is non-linear with a nearly exponential decaying diameter. Perturbing the mechanical features of the dividing cell by any number of mutations (particularly myosin II, cortexillin I, dynacortin, and racE) changes the furrow ingression dynamics, in some cases dramatically at the point of cross-over. Thus, the crossover is a highly significant parameter for the furrow ingression process and seems to strongly reflect features of the underlying mechanics. The second phase lasts until a thin bridge of diameter ~400 nm is formed. Phase 3 is marked by the bridge-dwelling phase in which the bridge does not thin appreciably as it awaits scission. In *Dictyostelium*, this phase is governed by a different genetic program [15,16], and in mammalian cells, this is the point when the ESCORT (ESCRT) complex proteins are thought to mediate final bridge separation [17,18].

A mechanical description of the cell during cytokinesis

To achieve a quantitative understanding of the dynamics of cytokinesis requires a mechanical description of the material properties of the cell (Figs. 1B,C). To this end, a number of models have been used, most of which assume that the cellular resistance to a stress exhibits both elastic and viscous components. Elastic behavior, which is a common assumption for solids, is one that obeys Hooke's law, in which the strain (deformation) is proportional to the stress. In contrast, the strain in a viscous material, a common model for fluids, depends on the *rate* of applied stress. Viscoelastic materials show a combination of the two extremes. Of course, in practice cells demonstrate considerably more complicated behavior which includes non-linear elasticity and strain stiffening and often with long-time viscous behavior [19–21].

Mechanical models of cells usually assume that the cell consists of two adjacent compartments in which an outer shell, formed by the membrane and underlying cortex, is predominantly elastic and encloses a mostly viscous cytoplasm (Fig. 1C). The membrane/cortex is characterized by its surface tension, which includes the physical properties of the membrane and the underlying cortex. If the coupling between the plasma membrane and cortex is loose then the cellular surface tension is not a simple addition of the tensions of plasma membrane and cortex. However, if the membrane and cortex are tightly coupled then total surface tension is the sum of the in-plane tension of the plasma membrane and the cortical tension [22]. Mechanical studies of cells treated with inhibitors of actin polymerization indicate that ~90% of the cortical mechanical properties are governed by the actin network [23–25], indicating that the contribution of the plasma membrane to the total tension is considerably lower than that of cortical tension (at least in *Dictyostelium*).

Cortical tension, T_{cortex}, is the apparent cell surface tension that can be attributed to mechanical stresses acting on the surface of the cell. It consists of two parts: active processes, such as myosin motors pulling on the actin network, and elastic deformations and other cortical flows. Stresses can act to deform the cell surface in two ways
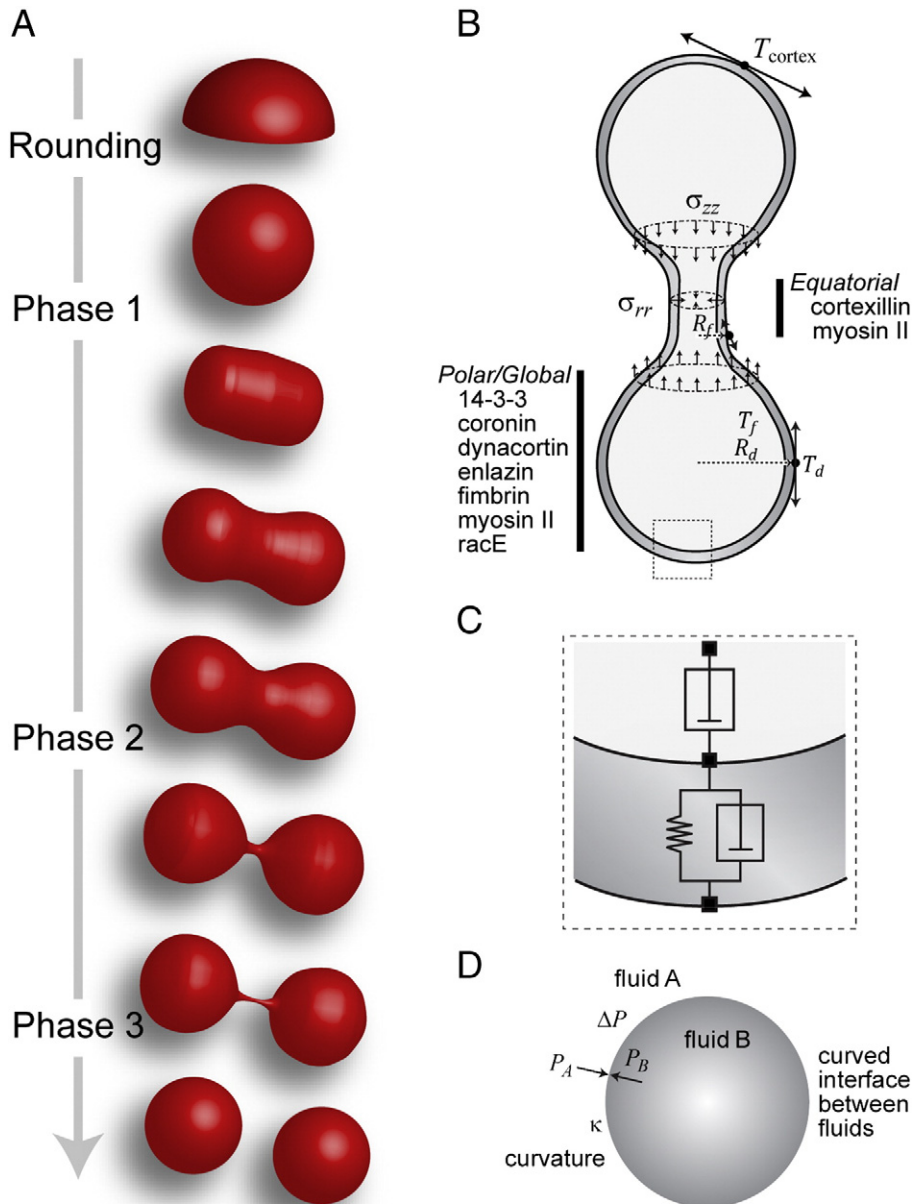
Fig. 1 – Mechanical properties during different phases of cytokinesis. A. Cell progression through cytokinesis can be characterized by a number of distinct morphological changes that correspond to different mechanical phases. After rounding, Phase 1 describes the change from a spherical to a cylindrical cell. Phase 2 is characterized by furrow ingression. Phase 3 is characterized by the thin bridge connecting the daughter cells. B. During cytokinesis, proteins such as myosin II and cortexillin localize to the cleavage furrow, while others are found globally or more concentrated at the poles. These localizations give rise to spatially dependent mechanical properties. Also shown are the different stresses (radial, σ_{rr}, and compressive, σ_{zz}) acting during cytokinesis as well as the spatially dependent cortical tensions (T_f and T_d at the furrow and daughter cells, respectively) which, when coupled to the local curvatures (arising from radii R_f and R_d) give rise to local Laplace-like pressures that help drive cytokinesis. C. A viscoelastic model of the cell encompasses a mostly viscous cytoplasm and a cortex that, though primarily elastic, also includes a viscous component [20]. D. The diagram depicts the Laplace pressure generated at the curved interface between fluid surfaces.

and different constants describe these deformations. These are the bending modulus (B) and stretch modulus (S_c) which are described as the resistance to deformation normal to the surface, and viscoelasticity in the plane tangential to the cell surface, respectively. These represent the energy costs needed to deform a cell. Which

of these two features that dominates during a specific cellular deformation can be determined by the characteristic length (l), given by: $l = (B/T_{cortex})^{1/2}$. For *Dictyostelium* cells, the measured values for B and T_{cortex} are 2×10^{-3} nN μm and 1 nN μm^{-1}, respectively [5,11]. Therefore, $l \approx 50$ nm, implying that for μm-scale cellular

deformations (*e.g.*, the width of a cleavage furrow) it is reasonable to consider that the energy cost from stretch will dominate.

The stretch modulus is caused by cortical actin filaments and crosslinkers, and is a strong predictor of amount of myosin II recruited to the cleavage furrow cortex [14,23]. The stretch modulus contributes to the cortical tension according to $T_{cortex} = \gamma_0 + S_C (A-A_0)/A_0$, where, γ_0 is the constant tension, A is the surface area and A_0 is the equilibrium surface area of the cortex [26,27]. Other related formulations have also been proposed where the cortical tension depends on the elasticity and thickness of the cortex. In this case, $T_{cortex} = \zeta\Delta\mu h + Eh (A-A_0)/A_0$, where $\zeta\Delta\mu$ is the active stress exerted on the cortical network, ζ is a coefficient relating the energy provided by ATP hydrolysis, $\Delta\mu$ is the active stress, E is the elastic modulus, and h is the thickness of the cortex [22,25].

During cytokinesis, cortical tension initially resists the deformation of the mother cell [12]. However, late in cytokinesis, cortical tension assists the furrow region to squeeze cytoplasm from the bridge into the two daughter cells. This is due to Laplace-like pressures, generated at the interface between fluid surfaces (Fig. 1D), acting on the cell [12]. Its magnitude is given by $P = \kappa T_{cortex}$, where κ is the curvature of the interface. For a sphere with radius R, the curvature is given by $2/R$; for a cylinder, $1/R$.

Active stresses acting during cytokinesis

Active stresses are generated by motor proteins and polymer assembly. Polymer assembly generates stress because of the force generated at the tip upon addition of polymer sub-units [22,28,29]. The force provided by this mechanism equals $f = (k_B T/\delta)\ln(k_+ c_A/k_-)$, where c_A is the free monomer concentration, k_+ and k_- are the kinetics of binding and release, respectively, and δ is the unit length increase due to the incorporation of a new sub-unit. During *Dictyostelium* cytokinesis, bulk actin polymerization occurs primarily at the poles. The actin nucleating factor Arp2/3 and its activators are found at the poles [30], suggesting that new actin assembly at the poles may contribute to propagation of stresses throughout the elastic cytoskeletal network [31].

The active stress (σ), generated by motors such as myosin II, is described by $\sigma = nF \times$ (duty ratio)$/SA$, where n is the number of heads in bipolar thick filament form, F is the force production per myosin II head, duty ratio is the fraction of myosin heads in the force-generating state as compared to the total number of available heads, and SA is the surface area of the cortex. Based on measurements on dividing *Dictyostelium* cells [12,14], the total quantity of myosin II (~100,000 hexamers), the force/head (4 pN), unloaded (no resistive force) duty ratio (0.6%), and the surface area of the cleavage furrow (75 μm^2), the predicted myosin II-generated radial stresses are estimated to be approximately 0.05 nN/μm^2 with a total force on the order of 4 nN. Other myosins, such as myosin I, also contribute to cortical tension [32] and at least one of these is localized to the polar cortex [33]. However, the roles of unconventional myosins in cytokinesis mechanics are not yet well studied.

Models for cleavage furrow ingression

The cleavage furrow cortex generates stresses [34,35]. Therefore, to understand the mechanics behind this stress generation and to build a model for cytokinesis it is necessary to characterize these stresses quantitatively. In 1972, Yoneda and Dan proposed one of the earliest models that used stresses and geometry to estimate the force required during furrow ingression [36]. The model uses two independent variables: the furrow radius and related geometry as well as the cortical tension to compute the minimum force required to stabilize intermediate shapes as the cell progresses through the different phases of cleavage furrow ingression. For *Dictyostelium*, this model predicts that a minimum force of 7 nN is required and this value closely matches the force that the experimentally measured accumulation of myosin II can provide [14].

A more recent model [37], in which the force at the contractile ring depends on the length of the bipolar thick filament, the length of the actin polymer and the circumference of the ring, estimates 20–30 fold lower forces than suggested by the Yoneda and Dan relationship and the measured myosin II amounts [14,36]. However, the authors point out that the effective length of the actin polymer could be much longer through crosslinking, and the linking of the actin filaments does indeed increase the theoretical stress generated by the system [37,38]. Indeed, the measured cellular concentrations of actin crosslinkers, the actin polymer density, and the measured stresses are consistent with a highly interconnected contractile network operating at the cleavage furrow cortex [5,12,39].

Zumdieck and co-workers developed a model for contractile ring constriction, which not only includes the contractile stresses, but also accounts for the effects of actin polymer turnover [36]. In this model, filament polymerization and depolymerization generate stresses when end-tracking cross-linkers are present. The latter suggests a possible explanation for cleavage furrow ingression in the absence of myosin II. Long-lived actin crosslinkers should increase the effective force by allowing forces to be transmitted through the network, whereas short-lived crosslinkers contribute an effective viscosity by slowing the contriction rate [5].

Because cytokinesis involves the deformation of the complete cell, furrow ingression is not just the result of contractility at the cell's equator. Therefore, the mechanics and dynamics of the entire cortex and cytoplasm must also be considered to account quantitatively for cytokinesis cell shape change. The cylinder-thinning model is one such analytical model that aims to incorporate all of these cellular domains to explain the dynamics of furrow ingression [12]. It incorporates cytoskeletal mechanics, cortical tension, Laplace pressure, viscoelasticity and viscosity. The model assumes that the outward flow of the cytoplasmic fluid is driven by Laplace-like pressures derived from the cortical tension of the furrow region, T_f, according to $\Delta P_f = T_f/R_f$, and radial stresses (σ_{rr}) from myosin II (Fig. 1B). This force is resisted by compressive stresses along the cylinder's long axis (σ_{zz}) that act at the end of the bridge. These compressive stresses also arise from Laplace-like pressure from the daughter cell cortices ($\Delta P_d = 2T_d/R_d$), and from the polar/global cortical contractions. The viscoelastic resistance of the cytoplasm further acts to dampen the flow of cytoplasm. The viscosity is non-linear being dependent on the relevant time-scale, length-scale and applied force to the cytoskeletal material. Based on dimensional analysis, the velocity (v) of bridge recoil is given by the ratio of tension at the furrow to the viscosity (μ) such that $v = T_f/3\mu$. For wild type *Dictyostelium* cells, an effective viscosity of ~0.35 nNs/μm^2 is calculated from the measured cortical tension of 1 nN/μm and recoil velocity of 1 μm/s. This compares with the largest force-dependent viscosity of 0.35 nNs/μm^2 measured for cells using magnetic rheometry [40]. This

model can account for the furrow ingression dynamics of wild type cells as well as several genetically modified cells (*e.g. myosin II* (*myosin II heavy chain, mhcA*) null, *racE* null and *dynacortin* RNAi hairpin cells) observed experimentally.

Paluch and colleagues [41] built upon the framework of Yoneda and Dan and the cylinder thinning model to develop a model of cytokinesis in mammalian cells. The main contribution of the proposed "soap bubble" model is that size differences between the poles result in pressure differences, creating a positive feedback, which accounts for their experimental observations of cell oscillations and instability in the shape of a dividing cell.

Recently, we also extended the cylinder-thinning model by carrying out a computational study of furrow ingression dynamics in which the cell shape changes were simulated using level set methodology [20,42]. This model utilizes only measured parameters and accounts for a range of cell division events: for example, adherent *vs.* non adherent cells or cells with or without myosin II contractile forces. The simulations demonstrate that traction-mediated protrusive forces or contractile forces due to myosin II are sufficient to initiate furrow ingression. However, the passive forces due to the cell's cortical tension and surface curvature are the primary drivers that allow the furrow to complete ingression. The principle role for cortical tension in driving furrow ingression has been further highlighted in a recent study of mammalian cytokinesis where a mutant nonmuscle myosin IIB, which is incapable of driving actin translocation, was able to support cytokinesis in cell culture cells and in cardiac myocytes of developing mouse hearts [43].

One further aspect of cytokinesis mechanics recently explored using models is the cell size-dependent scalability of actomyosin ring constriction. In *Caenorhabditis elegans* embryos, the rate of cytokinesis constriction depends on cell size, *i.e.* a cell with two times a diameter constricted at twice the rate implying that the rate of constriction is scalable with cell size [44]. This observation was extended to *Neurospora crassa* filamentous fungal cells [45], suggesting that scalability may be a property conserved among different cell types. In *N. crassa* cells, initial myosin II concentration correlates with cell size, but then this level remains constant during ring constriction. In contrast, in the *C. elegans* embryo, the myosin II density appears to be independent of cell size, but more total myosin II accumulates, due to the larger circumference. In both cases, it is proposed that the increased contraction rates are due to the greater amounts of myosin motors associated with the rings. However, to explain fully the scalability, other implications of cell size must also be accounted for, such as the dependency of surface curvature on radius and the correlation of daughter cell radius on the initial mother cell radius, all of which may affect furrow ingression dynamics.

Mechanosensing and mechanical feedback during cytokinesis

Because of the importance of achieving cell division successfully and because cytokinesis is primarily a mechanical phenomenon, we hypothesized that feedback mechanisms could play a role in minimizing the effect of mechanical disturbances by regulating the contractile apparatus and providing shape control. Using micropipette aspiration, we applied stresses to the surface of cells that are similar in magnitude (0.1–1.0 nN/μm^2) to those that dividing cells generate at the cleavage furrow cortex [46]. These stresses induced myosin II and the actin crosslinking protein cortexillin I (two cleavage furrow proteins) to accumulate in a coordinated fashion at the micropipette (Fig. 2). Further experiments demonstrated that this mechanosensation depended on the force amplification by the myosin II lever arm and the myosin II bipolar thick filament assembly and disassembly dynamics [13].

To explain the mechanosensory step, we developed a dynamical model of BTF assembly–disassembly dynamics [13]. Kinetic simulations based on this model showed that a crucial step allowing for accumulation of myosin II at the site of a mechanosensory feedback response is the first step of the BTF assembly pathway: the conversion of assembly incompetent monomers to
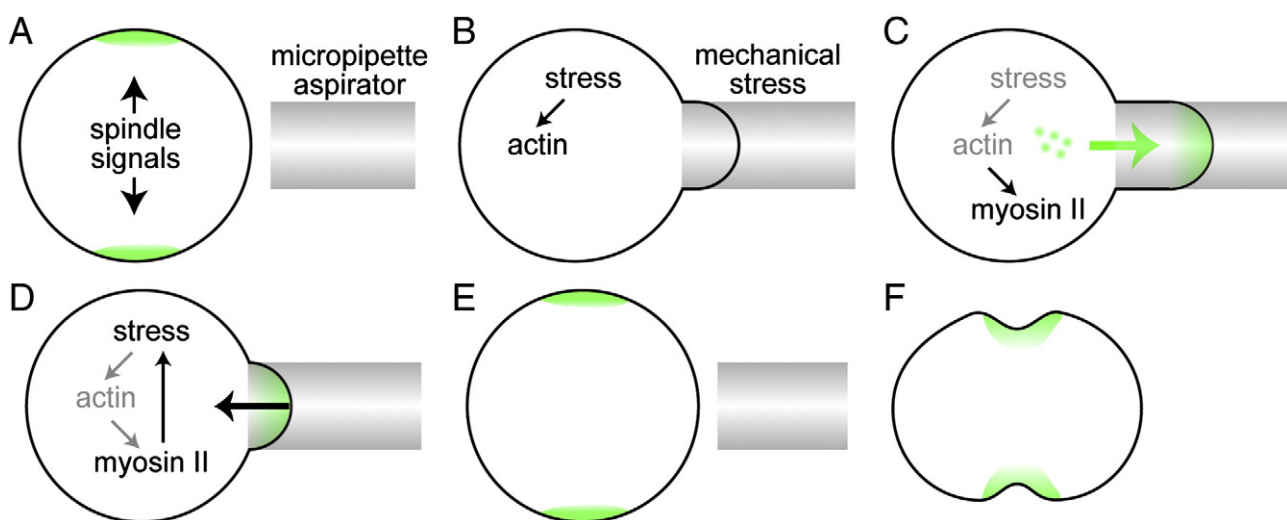

Fig. 2 – A mechanosensitive system regulates cytokinesis. A. During cytokinesis, signals believed to come from the spindle direct cortical proteins such as a myosin II or cortexillin to the future site of the cleavage furrow. B. External stresses, such as those imposed by a micropipette aspirator can cause changes in morphology. C. Stresses in the actin can give rise to cooperative recruitment of myosin II/cortexillin to the site of stress [13,48]. D. Recruited myosin II works against the external stress enabling the cell to exit the micropipette (E) at which point normal division can proceed (F).

assembly competent monomers [13]. The BTF assembly properties unveiled by the model suggests several possible mechanosensitive assembly mechanisms. First, a myosin heavy chain phosphatase could be activated or a myosin heavy chain kinase (MHCK) might be locally inactivated. Either of these processes could shift the local ratio of assembly-competent to incompetent monomers. The inactivation of a myosin heavy chain kinase seems unlikely since one isoform, MHCKC, which tracks its myosin II heavy chain substrate, accumulates in response to mechanical stress [47,48]. Further, any model that explains the mechanosensitive accumulation must account for the lever-arm length dependency [13]. Therefore, we proposed another possible mechanism [48] in which myosin motor domains in local mini-BTFs are stabilized in the transition state by mechanical stress, additional unassembled myosin monomers may bind the actin filament through cooperative interactions between motor domains along the filament. Once these motors are localized along a filament, the monomers may then directly incorporate into the BTF. We developed a multi-scale model that incorporates known biochemical activities, including cooperative myosin–actin binding, thick filament assembly dynamics, and *in vivo* concentrations and stresses to account for mechanosensitive myosin II accumulation [48]. This model accounts for the sigmoidal binding curves and two-dimensional cluster formation observed in biochemical assays. Moreover, the model could account for possible hetero-cooperativity between myosin II and cortexillin I. Most significantly, by incorporating the kinetics of myosin BTF assembly, the model could account for the three-dimensional pattern of the cooperative accumulation of myosin observed experimentally during MPA.

Concluding remarks

Cytokinesis proceeds as a result of an integrated control system characterized by mechanical–biochemical feedback loops [39]. Therefore, a quantitative study of the mechanics of this control system provides a thorough knowledge on how cells undergo stable cell shape changes and thereby complete error-free cytokinesis in a wide variety of mechanical environments such as tissues and/or organs. Furthermore, cytokinesis research also sheds light on cancer cell biology, as many cancer genes encode proteins that play significant roles in cytokinesis. Ultimately, understanding how these proteins contribute to the mechanics and regulation of cytokinesis may aid in the development of novel therapeutic strategies for cancer treatment.

Acknowledgments

REFERENCES

[1] J.M. Mitchison, M.M. Swann, The mechanical properties of the cell surface: II. The unfertilized sea-urchin egg, J. Exp. Biol. 31 (1954) 461–472.

[2] J.M. Mitchison, M.M. Swann, The mechanical properties of the cell surface: III. The sea-urchin egg from fertilization to cleavage, J. Exp. Biol. 32 (1955) 734–750.

[3] Y. Hiramoto, Mechanical properties of sea urchin eggs II. Changes in mechanical properties from fertilization to cleavage, Exp. Cell Res. 32 (1963) 76–88.

[4] P. Kunda, A.E. Pelling, T. Liu, B. Baum, Moesin controls cortical rigidity, cell rounding, and spindle morphogenesis during mitosis, Curr. Biol. 18 (2008) 91–101.

[5] E.M. Reichl, Y. Ren, M.K. Morphew, M. Delannoy, J.C. Effler, K.D. Girard, S. Divi, P.A. Iglesias, S.C. Kuo, D.N. Robinson, Interactions between myosin and actin crosslinkers control cytokinesis contractility dynamics and mechanics, Curr. Biol. 18 (2008) 471–480.

[6] A. Lucero, C. Stack, A.R. Bresnick, C.B. Shuster, A global, myosin light chain kinase-dependent increase in myosin II contractility accompanies the metaphase-anaphase transition in sea urchin eggs, Mol. Biol. Cell 17 (2006) 4093–4104.

[7] D.N. Robinson, J.A. Spudich, Dynacortin, a genetic link between equatorial contractility and global shape control discovered by library complementation of a *Dictyostelium discoideum* cytokinesis mutant, J. Cell Biol. 150 (2000) 823–838.

[8] C. Janetopoulos, J. Borleis, F. Vazquez, M. Iijima, P. Devreotes, Temporal and spatial regulation of phosphoinositide signaling mediates cytokinesis, Dev. Cell 8 (2005) 467–477.

[9] A.S. Maddox, K. Burridge, RhoA is required for cortical retraction and rigidity during mitotic cell rounding, J. Cell Biol. 160 (2003) 255–265.

[10] M.P. Stewart, J. Helenius, Y. Toyoda, S.P. Ramanathan, D.J. Muller, A.A. Hyman, Hydrostatic pressure and the actomyosin cortex drive mitotic cell rounding, Nature 469 (2011) 226–230.

[11] E.M. Reichl, J.C. Effler, D.N. Robinson, The stress and strain of cytokinesis, Trends Cell Biol. 15 (2005) 200–206.

[12] W. Zhang, D.N. Robinson, Balance of actively generated contractile and resistive forces controls cytokinesis dynamics, Proc. Natl. Acad. Sci. U. S. A. 102 (2005) 7186–7191.

[13] Y. Ren, J.C. Effler, M. Norstrom, T. Luo, R.A. Firtel, P.A. Iglesias, R.S. Rock, D.N. Robinson, Mechanosensing through cooperative interactions between myosin II and the actin crosslinker cortexillin I, Curr. Biol. 19 (2009) 1421–1428.

[14] D.N. Robinson, G. Cavet, H.M. Warrick, J.A. Spudich, Quantitation of the distribution and flux of myosin-II during cytokinesis, BMC Cell Biol. 3 (2002) 4.

[15] A. Nagasaki, T.Q. Uyeda, DWWA, a novel protein containing two WW domains and an IQ motif, is required for scission of the residual cytoplasmic bridge during cytokinesis in *Dictyostelium*, Mol. Biol. Cell 15 (2004) 435–446.

[16] T. Liu, J.G. Williams, M. Clarke, Inducible expression of calmodulin antisense RNA in *Dictyostelium* cells inhibits the completion of cytokinesis, Mol. Biol. Cell 3 (1992) 1403–1413.

[17] J.G. Carlton, J. Martin-Serrano, Parallels between cytokinesis and retroviral budding: a role for the ESCRT machinery, Science 316 (2007) 1908–1912.

[18] H.H. Lee, N. Elia, R. Ghirlando, J. Lippincott-Schwartz, J.H. Hurley, Midbody targeting of the ESCRT machinery by a noncanonical coiled coil in CEP55, Science 322 (2008) 576–580.

[19] J. Stricker, T. Falzone, M.L. Gardel, Mechanics of the F-actin cytoskeleton, J. Biomech. 43 (2010) 9–14.

[20] L. Yang, J.C. Effler, B.L. Kutscher, S.P. Sullivan, D.N. Robinson, P.A. Iglesias, Modeling cellular deformations using the level set formalism, BMC Syst. Biol. 2 (2008) 68.

[21] E. Evans, A. Yeung, Apparent viscosity and cortical tension of blood granulocytes determined by micropipet aspiration, Biophys. J. 56 (1989) 151–160.

[22] A.G. Clark, E. Paluch, Mechanics and regulation of cell shape during the cell cycle, Results Probl. Cell Differ. 53 (2011) 31–73.

[23] K.D. Girard, C. Chaney, M. Delannoy, S.C. Kuo, D.N. Robinson, Dynacortin contributes to cortical viscoelasticity and helps define the shape changes of cytokinesis, EMBO J. 23 (2004) 1536–1546.

[24] K.D. Girard, S.C. Kuo, D.N. Robinson, *Dictyostelium* myosin II mechanochemistry promotes active behavior of the cortex on long time scales, Proc. Natl. Acad. Sci. U. S. A. 103 (2006) 2103–2108.

[25] J.Y. Tinevez, U. Schulze, G. Salbreux, J. Roensch, J.F. Joanny, E. Paluch, Role of cortical tension in bleb growth, Proc. Natl. Acad. Sci. U. S. A. 106 (2009) 18581–18586.

[26] J. Derganc, B. Božic, S. Svetina, B. Žekš, Stability analysis of micropipette aspiration of neutrophils, Biophys. J. 79 (2000) 153–162.

[27] D.N. Robinson, Y.-S. Kee, T. Luo, A. Surcel, Understanding how dividing cells change shape, in: E. Egelman (Ed.), Comprehensive Biophysics, vol. 7, Elsevier, Amsterdam, 2012, pp. 48–72.

[28] D.R. Kovar, T.D. Pollard, Insertional assembly of actin filament barbed ends in association with formins produces piconewton forces, Proc. Natl. Acad. Sci. U. S. A. 101 (2004) 14725–14730.

[29] T. Luo, D.N. Robinson, The role of the actin cytoskeleton in mechanosensation, in: A. Kamkin, I. Kiseleva (Eds.), Mechanosensitivity in Cells and Tissues: Mechanosensitivity and Mechanotransduction, vol. 4, Springer-Verlag, New York, 2011, pp. 25–65.

[30] R. Insall, A. Muller-Taubenberger, L. Machesky, J. Kohler, E. Simmeth, S.J. Atkinson, I. Weber, G. Gerisch, Dynamics of the Dictyostelium Arp2/3 complex in endocytosis, cytokinesis, and chemotaxis, Cell Motil. Cytoskeleton 50 (2001) 115–128.

[31] S. Yumura, Y. Fukui, Spatiotemporal dynamics of actin concentration during cytokinesis and locomotion in Dictyostelium, J. Cell Sci. 111 (1998) 2097–2108.

[32] J. Dai, H.P. Ting-Beall, R.M. Hockmuth, M.P. Sheetz, M.A. Titus, Myosin I contributes to the generation of resting cortical tension, Biophys. J. 77 (1999) 1168–1176.

[33] Y. Fukui, T.J. Lynch, H. Brzeska, E.D. Korn, Myosin I is located at the leading edges of locomoting Dictyostelium amoebae, Nature 341 (1989) 328–331.

[34] R. Rappaport, Cell division: direct measurement of maximum tension exerted by furrow of echinoderm eggs, Science 156 (1967) 1241–1243.

[35] K. Burton, D.L. Taylor, Traction forces of cytokinesis measured with optically modified elastic substrata, Nature 385 (1997) 450–454.

[36] M. Yoneda, K. Dan, Tension at the surface of the dividing sea-urchin egg, J. Exp. Biol. 57 (1972) 575–587.

[37] A.E. Carlsson, Contractile stress generation by actomyosin gels, Phys. Rev. E: Stat. Nonlin. Soft Matter Phys. 74 (2006) 051912.

[38] N.L. Dasanayake, P.J. Michalski, A.E. Carlsson, General mechanism of actomyosin contractility, Phys. Rev. Lett. 107 (2011) 118101.

[39] A. Surcel, Y.-S. Kee, T. Luo, D.N. Robinson, Cytokinesis through biochemical–mechanical feedback loops, Semin. Cell Dev. Biol. 21 (2010) 866–873.

[40] W. Feneberg, M. Westphal, E. Sackmann, Dictyostelium cells' cytoplasm as an active viscoplastic body, Eur. Biophys. J. 30 (2001) 284–294.

[41] J. Sedzinski, M. Biro, A. Oswald, J.Y. Tinevez, G. Salbreux, E. Paluch, Polar actomyosin contractility destabilizes the position of the cytokinetic furrow, Nature 476 (2011) 462–466.

[42] C.C. Poirier, W.P. Ng, D.N. Robinson, P.A. Iglesias, Deconvolution of the cellular force-generating subsystems that govern cytokinesis furrow ingression, PLoS Comput. Biol. 8 (2012) e1002467, doi:10.1371/journal.pcbi.1002467.

[43] X. Ma, M. Kovacs, M.A. Conti, A. Wang, Y. Zhang, J.R. Sellers, R.S. Adelstein, Nonmuscle myosin II exerts tension but does not translocate actin in vertebrate cytokinesis, Proc. Natl. Acad. Sci. U. S. A. 109 (2012) 4509–4514.

[44] A. Carvalho, A. Desai, K. Oegema, Structural memory in the contractile ring makes the duration of cytokinesis independent of cell size, Cell 137 (2009) 926–937.

[45] M.E. Calvert, G.D. Wright, F.Y. Leong, K.H. Chiam, Y. Chen, G. Jedd, M.K. Balasubramanian, Myosin concentration underlies cell size-dependent scalability of actomyosin ring constriction, J. Cell Biol. 195 (2011) 799–813.

[46] J.C. Effler, Y.-S. Kee, J.M. Berk, M.N. Tran, P.A. Iglesias, D.N. Robinson, Mitosis-specific mechanosensing and contractile protein redistribution control cell shape, Curr. Biol. 16 (2006) 1962–1967.

[47] S. Yumura, M. Yoshida, V. Betapudi, L.S. Licate, Y. Iwadate, A. Nagasaki, T.Q. Uyeda, T.T. Egelhoff, Multiple myosin II heavy chain kinases: roles in filament assembly control and proper cytokinesis in Dictyostelium, Mol. Biol. Cell 16 (2005) 4256–4266.

[48] T. Luo, K. Mohan, V. Srivastava, Y. Ren, P.A. Iglesias, D.N. Robinson, Understanding the cooperative interaction between myosin II and actin crosslinkers mediated by actin filaments during mechanosensation, Biophys. J. 102 (2012) 238–247.